Applying energy autonomous robots for dike inspection *

Douwe Dresscher, Theo J.A. de Vries, and Stefano Strmigioli

Robotics and Mechatronics group
Centre for Telematics and Information Technology
University of Twente
P.O. Box 217, NL-7500 AE Enschede, The Netherlands
Email: D.Dresscher@ieee.org, S.Stramigioli@ieee.org

Abstract. This article presents an exploratory study of an energy-autonomous robot that can be deployed on the Dutch dykes. Based on theory in energy harvesting from sun and wind and the energy-cost of locomotion an analytic expression to determine the feasible daily operational time of such a vehicle is composed. The parameters in this expression are identified using lab results and weather statistics. After an evaluation of the "Energy autonomous robot in the Netherlands" case, the results are generalised by looking at the effects of varying the assumptions. Based on this work, three conclusions can be drawn. Firstly, it is realistic to have an energy-autonomous walking dyke robot in the Netherlands. Secondly, the use of solar panels is probably not feasible if the amount of solar energy that is available is much less than assumed in the study. Finally, in this case study, the inclusion of a wind turbine typically offers a slight benefit. Furthermore, it gives a significant benefit in the months where the incident power of the sun is low, thus allowing a reasonable operational time during the winter.

1 Introduction

The Netherlands - the name itself means "low countries" - is a geographically low lying country. More than 60% of the land lies below sea level, including the densely populated "Randstad" region which is encircled in red. Over 7.000.000 people live and work in this region, which is a little more than 40% of the Dutch population. Without effective flood defences, the parts that lie below sea level would frequently (if not permanently) be subjected to flooding. This makes it important for the Dutch to keep their flood defences in good shape and up-to-date. A major breach would be a disaster in many ways.

An important part of the flood defence system consists of dykes. Recent (2003, 2004) dyke failures have shown that knowledge about the flood-defence systems is insufficient to always prevent flooding. The goal of the ROSE project is to develop a 'team' of robotic walkers that will function as an autonomous

* This work was financed by the Dutch Technology Foundation STW under grant 10550.

early-warning system by acquiring data about the composition, consistency and condition of dykes.

Energy autonomy implies that the robot takes care of its own energy supply. Energy sources available to a robot in an outdoor environment may include unrefined biomass, sun and wind. Of these, robotic energy harvesting from unrefined biomass has not yet progressed beyond the laboratory, although the research is promising [4, 13]. By contrast, equipment to harvest energy from sun and wind has been available COTS (Commercially Off The Shelf) for several decades and is continually improving. For this reason, this work focusses on energy autonomous robot that uses solar and/or wind energy.

This article presents an exploratory study of an energy-autonomous robot that can be deployed on the Dutch dykes. We start by giving some background information on energy harvesting from sun and wind and the energy-cost of locomotion. This information is combined in an analytic expression to determine the feasible daily operational time of such a vehicle. The parameters in this expression are identified for a dyke robot in the Netherlands to which the theory will be applied. Next, the results are generalised by looking at the effects of varying the assumptions. The work closes with a discussion of the results and drawing conclusions.

2 Theoretical background

To evaluate the energy autonomy of a robot, the achievable operational (working) time per day can be used as a measure. The operational time per day can be determined from the energy that can be harvested in a day and the average power consumption of the robot by applying the following reasoning. Since we do not add/remove energy to/from the system in any other way then by harvesting, the maximum energy that the system can consume, E_{cons}, is equal to the energy that the system harvests, E_{harv}.

$$E_{cons} = E_{harv} \tag{1}$$

where the energy that the system consumes is equal to the product of the average power consumption, $\bar{P}_{total}$, and the operational time per day, T_{op}: $E_{cons} = T_{op}\bar{P}_{total}$ such that $T_{op}\bar{P}_{total} = E_{harv}$ or:

$$T_{op} = \frac{E_{harv}}{\bar{P}_{total}} \tag{2}$$

In the following two sections, the derivation of the harvested energy per day and average power consumption is discussed.

2.1 Harvested energy per day

For this work, two types of energy harvesting are considered: energy harvesting from solar energy and energy harvesting from wind energy. The total amount

of harvested energy is equal to the sum of the harvested solar energy, E_s, and harvested wind energy, E_{wt}:

$$E_{harv} = E_s + E_{wt} \tag{3}$$

From weather statistics, the average effective incident energy per square metre per day, $\bar{E}_{sun}\{Whm^{-2}\}$, can be obtained. Using this information, the average energy generated by the solar panels, $\bar{E}_s\{Wh\}$, can be calculated based on the surface area $S_s\{m^2\}$ and the efficiency $\gamma_s\{\}$ of the solar panel:

$$\bar{E}_s = S_s \gamma_s \bar{E}_{sun} \tag{4}$$

For the calculation of the energy that can be harvested from the wind, the average wind speed over 24 hours, $\bar{v}_{wind}\{ms^{-1}\}$, is available from weather statistics. Using this information, Betz' law [1] can be used to calculate the maximum average power generation under ideal conditions, using a wind turbine, $\bar{P}_w\{W\}$:

$$\bar{P}_w = 0.5 \rho_{air} \bar{v}^3_{wind} S_w C_p \tag{5}$$

where $\rho_{air}\{kgm^{-3}\}$ is the density of the air, $S_w\{m^2\}$ the effective surface area of the wind turbine (sectional area) and $C_p\{\}$ the power coefficient of the wind turbine. Using this, the amount of wind energy that is harvested in a day can be calculated:

$$E_{wt} = 24\bar{P}_w = 12 \rho_{air} \bar{v}^3_{wind} S_w C_p \tag{6}$$

The total energy that is harvested in a day is now equal to:

$$E_{harv} = E_s + E_{wt} = 24 S_s \gamma_s \bar{P}_{sun} + 12 \rho_{air} \bar{v}^3_{wind} S_w C_p \tag{7}$$

2.2 Average power consumption

The total power consumption, $\bar{P}_{total}$, can be split into the power consumption of the robot's locomotion system ($\bar{P}_l$) and the power consumption from other equipment ($\bar{P}_o$):

$$\bar{P}_{total} = \bar{P}_l + \bar{P}_o \tag{8}$$

The power consumption of the robot's locomotion system can be calculated using a frequently used measure for the power consumption of a locomotion system, namely the specific resistance as first described by [2]. The specific resistance $\epsilon\{\}$ is defined as the ratio of power used for locomotion $P_l\{W\}$ and the product of the weight $m\{kg\}$, earth's gravitational acceleration $g\{ms^{-2}\}$ and the maximum speed $v_{max}\{ms^{-1}\}$, such that:

$$\epsilon = \frac{P_l}{mgv_{max}} \tag{9}$$

This can be rewritten to:

$$P_l = \epsilon mgv_{max} \tag{10}$$

such that, when given a certain specific resistance of a locomotion system for a certain maximum speed and mass, the power consumption can be calculated.

Splitting the total mass, m, into the mass of the locomotion system, m_l; the solar panels, m_s; the wind turbine, m_w; and the mass of other equipment, m_o, results in:

$$P_l = \epsilon(m_l + m_s + m_w + m_o)gv_{max} \tag{11}$$

Let us assume that, when changing the surface area of a wind turbine, the change in depth is negligible. Then, the mass of the wind turbine, m_w, is approximately linearly dependent on the surface area of the wind turbine, S_w:

$$m_w = \eta_w S_w, \tag{12}$$

where η_w represents the planar density of the wind turbine. It is reasonable to assume that such an approximation also exists for the weight of the solar panels:

$$m_s = \eta_s S_s \tag{13}$$

where η_s is the density of the solar panels. Now:

$$P_l = \epsilon(m_l + \eta_s S_s + \eta_w S_w + m_o)gv_{max} \tag{14}$$

such that the total power consumption is equal to:

$$\bar{P}_{total} = \epsilon(m_l + \eta_s S_s + \eta_w S_w + m_o)gv_{max} + \bar{P}_o \tag{15}$$

2.3 An analytic expression for the operational time per day

Combining equations 2, 7 and 15 results in:

$$T_{op} = \frac{S_s \gamma_s \bar{E}_{sun} + 12\rho_{air}\bar{v}^3_{wind} S_w C_p}{\epsilon(m_l + \eta_s S_s + \eta_w S_w + m_o)gv_{max} + p_o} \tag{16}$$

which enables the relation between solar panel and/or wind turbine surface area and the operational time to be studied.

3 Parameter identification

Using equation 16, the operational time per day can be evaluated for an area of solar panel and wind turbine surface. The next step is to determine the other parameters used in equation 16 based on the case of a dyke inspection robot in the Netherlands. In this section, weather statistics and experimental results that have been achieved for both energy harvesting and locomotion are used to give a value to the parameters. Equipment other than the locomotion system and harvesting equipment is not considered; this implies $P_o = 0$ and $m_o = 0$.

3.1 Solar energy harvesting

As mentioned earlier, the study concerns a robot that will be deployed in the Netherlands and the average incident solar energy is used to obtain a realistic value for $\bar{P}_{sun}$. Fig. 1a shows the average solar energy (Whm^{-2}) that is incident per day, for each month of the year, in blue. Fig. 1b shows the average solar energy (Whm^{-2}) that is incident per day, for several locations in the Netherlands, in blue.

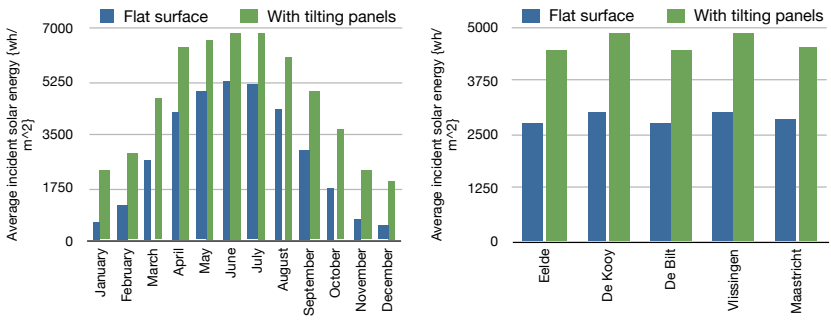

(a) Average incident solar energy per month in the Netherlands.

(b) Average incident solar energy for several locations in the Netherlands.

Fig. 1: Average incident solar energy in the Netherlands. The figures are shown for a flat surface (source: [8–11]) and an optimally tilted surface.

These numbers represent the incident energy on a flat surface and may be further increased by tilting the panels such that the surface is normal to the sun's rays (for details on the calculations, please refer to [16]). By applying this correction, we obtain incident energy as shown in green. For the case study, the average of these values is used, which is equal to 4334 Whm^{-2}. When the results are generalised later in this paper, monthly and geographical variations are evaluated.

The maximum theoretically achievable efficiency of solar cells is defined by the thermodynamic limit and is equal to 86% [12]. However, current levels are at 37.5% for InGaP/GaAs/InGaAs cells in a lab environment and 28.5% for GaAs (thin film) cells in commercially available modules [3]. Commercially available GaAs (thin film) modules can have a efficiency of 23.5%; this is 82% lower than the cell efficiency. The planar density of current state-of-the-art silicium panels is around $2.2kgm^{-2}$ [15].

In this study, we look at the opportunities offered by currently commercially available modules ($\gamma_s = 0.235$ and $\eta_s = 2.2$).

3.2 Wind energy harvesting

To obtain the average wind speed, average measurements are used as well. Figure 2a shows the average wind speed (ms^{-1}) in the Netherlands, for each month of the year. Fig. 2b shows the average wind speed for various locations in the Netherlands.

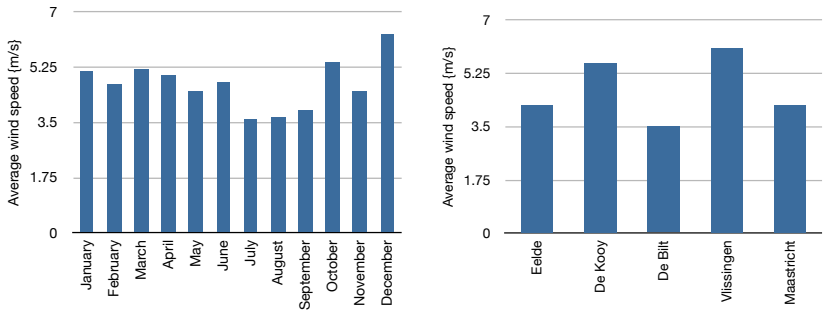

(a) Average wind speed in the Netherlands, for each month of the year.

(b) Average wind speed in the Netherlands, for each month of the year.

Fig. 2: verage wind speed in the Netherlands (source: [8–11])

For the study, the average of these values is used, which is equal to 4.78 ms^{-1}. When the results are generalised later in this paper, monthly and geographical variations are evaluated. The density of air, ρ_{air}, at $10°C$ is $1.25kgm^{-3}$.

The maximum theoretically achievable efficiency at which an idealised model of a wind turbine can convert the kinetic energy of wind to useful power is defined by Betz's coefficient and is equal to 0.59 [6]. Currently, the measured power coefficient is in the range 0.4-0.5 [7]. The problem is that currently available wind turbines are large and are not designed for mobile applications. Therefore, it is difficult to say if this number is realistic for a smaller model. However, for this study, we assume that it is realistic to have such a power coefficient for a smaller model. We use $C_p = 0.45$ and look at the implications of applying this assumption when the results are generalised later in this paper.

Currently available wind turbines are not designed for mobile applications and are therefore not optimised for low mass. For mobile applications, it is desirable to have a light turbine with a planar density of (say) 10kg per square metre of surface area. It is assumed that such a wind turbine is available ($\eta_w = 10kg$), and the implications of this assumption will be discussed when the results are generalised later in this paper.

3.3 Locomotion energy consumption

Many legged robots have been developed over the years. To identify a realistic set of parameters for the locomotion system, a state-of-the-art example is used.

In [5], the specific resistance of a range of vehicles. Among these is Scout II ([14]) which is a state-of-the-art multi-legged robots.

The locomotion system of the Scout II is, with a specific resistance of 1 at a velocity of $1\frac{m}{s}$, one of the most energy-efficient multi-legged walking systems currently available . Although these are experimental results from a lab environment, it is assumed that it is possible to locomote with this efficiency outside the lab, and therefore, the locomotion system of the Scout II robot is used as an example locomotion system in this case study. Therefore, ϵ is equal to 1, v_{max} is equal to $1ms^{-1}$ and m_l is equal to $25kg$ (including batteries and electronics)[14]. For the gravitational acceleration, g, a value of $9.81ms^{-2}$ is used.

3.4 Temporary energy storage

Depending on the short-term fluctuations in energy harvesting during operations, the robot needs to be equipped with temporary energy-storage capabilities in the form of batteries. For this analysis, it is assumed that the amount of battery storage with which the Scout II robot is equipped is sufficient to achieve this goal.

4 Exploratory study

Once the parameters have been identified, they can by substituted in equation 16. This results in the following expression:

$$T_{op} = \frac{1018.49S_s + 737.2S_w}{245.25 + 21.58S_s + 98.1S_w}, \tag{17}$$

such that the (yearly average) operational time per day can be expressed as a function of the solar panel and wind turbine surface area. When plotting the yearly average operational time per day as a function of the surface area of the solar panel and/or wind turbine, Fig. 3 is obtained; where the horizontal axis represents the area of solar panels/ wind turnbines and the vertical axis the operational time. For this case study, we assume that the robot can carry up to twice its top surface in solar panels; for the Scout II robot, this is $1.637m^2$ of solar panel, and a wind turbine with a radius of the length of the robot body at most; this results in a maximum surface of $0.55m^2$ for the Scout II robot.

From this, it can be seen that it is always beneficial to include solar panels when applying a wind-turbine (Fig. 3b). In addition, it shows that up to a certain amount of solar panel surface area, it is beneficial to include a wind turbine when applying solar panels (Fig. 3a). This boundary is at $2.15m^2$ of solar panel surface area. If the solar panel surface area is larger than $2.15m^2$, the presence of a wind turbine decreases the operational time. A wind turbine offers an improvement in the feasible operational time per day. However, if the maximum amount of solar panel surface is applied, the addition of a wind turbine offers only a small improvement - from 5.96 to 6.21 hours per day - .

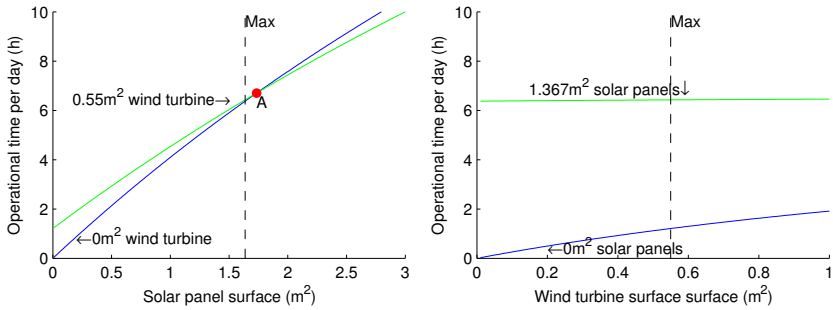

(a) The operational time per day vs the solar panel surface area in the case of no wind-turbine (in blue) and the case of a $0.55m^2$ wind turbine (in green).

(b) The operational time per day vs the wind turbine surface area in the case of no solar panels (in blue) and the case of a $1.637m^2$ wind turbine (in green).

Fig. 3: Case evaluation. Point A in the left figure is the point where there is no change in operational time with the addition of a wind-turbine, the area left of point A is the area where the addition of a wind turbine is beneficial and the area to the right of point A is the area where the addition of wind turbine is not beneficial. The black, dashed line marks the maximum solar panel surface for this study.

5 Generalisation of the results

In this study, assumptions are made regarding the parameters in equation 16. Since it is likely that a variation to these assumptions will apply in practise, the effect of variations to these assumptions is discussed in this section.

Fig. 4a shows the effect of varying the assumption about the efficiency of the solar panels.

Fig. 4b shows the effect of varying the assumption about the efficiency of wind turbine. It shows that when the efficiency of the wind turbine drops below 0.36, it is no longer beneficial to have a wind turbine when the maximum amount amount solar panels is applied.

Figures 5a and 5b show the result of a variation in the amount of incident solar energy and wind speed, respectively.

As shown in Figures 1a and 2a, the wind speed and incident solar energy change over the year; Fig. 6a shows how this affects the operational time per day. The figure shows that the inclusion of a $0.55m^2$ wind turbine reduces the operational time per day for most months. However, it also shows that it improves the operational time per day for the months with the lowest operational time per day. Without a wind turbine, the operational time ranges between 2.6 hours and 8.8 hours per day, while it ranges from 3.6 hours and 8.4 hours per day with a $0.55m^2$ wind turbine.

Figures 1b and 2b show that the wind speed and incident solar energy differ for different locations; Fig. 6b shows how this affects the operational time per

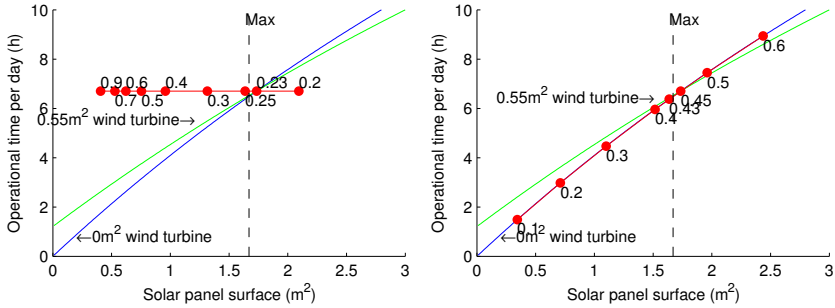

(a) Variations of the solar-panel efficiency γ_s.

(b) Variations of the wind-turbine efficiency C_p.

Fig. 4: A variation of Fig. 3 with the addition of the red line that shows how point A moves with variations of the solar-panel efficiency γ_s (left) and wind-turbine efficiency C_p (right), the red dots represent the specific values that are given alongside.

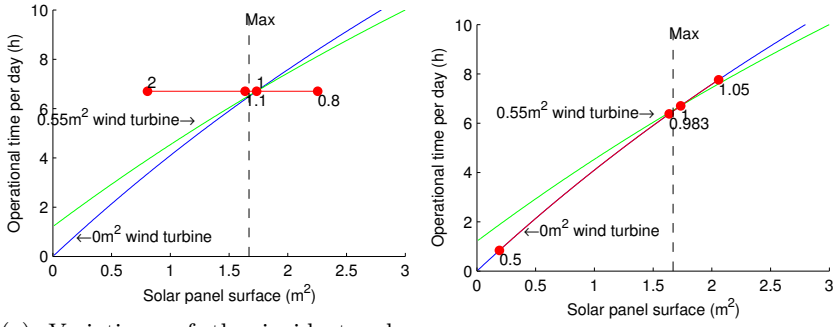

(a) Variations of the incident solar energy $\bar{E}_{sun}$.

(b) Variations of the wind speed $\bar{v}_{wind}$.

Fig. 5: Variations of Fig. 3 with the addition of the red line that shows how point A moves with variations of the incident solar energy $\bar{E}_{sun}$ and wind speed $\bar{v}_{wind}$. The red points represend the specific values that are given alongside.

day. For the regions "Eelde", "De Bilt" and "Maastricht", the addition of a wind turbine has a negative effect to the average operational time while it has a positive effect in the regions "De Kooy" and "Vlissingen".

The effect of applying a different assumption on the weight of the wind turbine and solar panels result in Figures 7a and 7b. Fig. 7a shows that if the solar panels are heavier, it it has a more significant effect on the operational time per day than if lighter solar panels are used. Fig. 7b shows that if the wind turbine planar density is more than $13kg/m^2$, it is no longer beneficial to include a wind turbine if the maximum area of solar panels is applied.

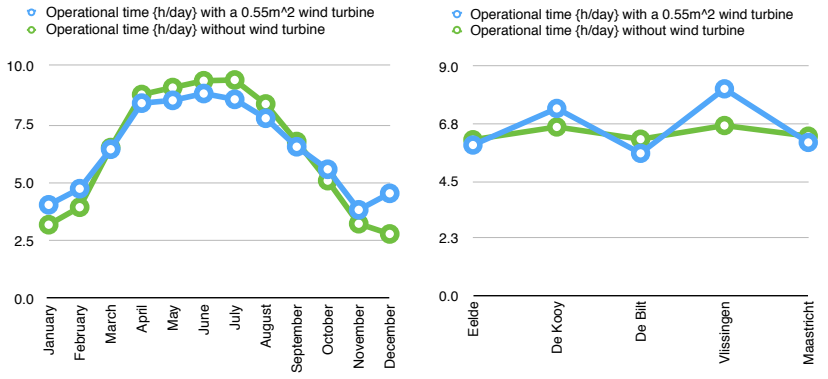

(a) Monthly varations

(b) Geographical variations

Fig. 6: The effect on monthly and geographical variations in incident solar energy and wind speed on the operational time per day for two situations: a $0.55m^2$ wind turbine and no wind turbine. For both situations, the maximum ($1.64m^2$) amount of solar panel surface is assumed.

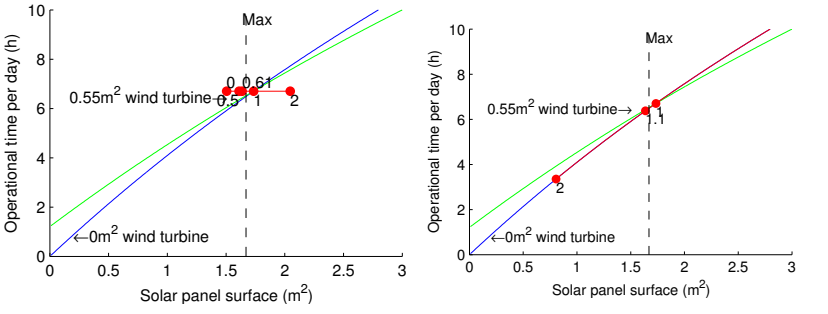

(a) Variations of solar panel weight per square metre η_s.

(b) Variations of the wind turbine weight per square metre η_w.

Fig. 7: A variation of Fig. 3 with the addition of the red line that shows how point A moves with variations solar panel weight per square metre η_s and wind turbine weight per square metre η_w, the red dots represent the specific values that are given alongside multiplied by the amount of weight per square metre as used in the study.

Another parameter that is interesting to vary is the total mass of the locomotion system, including batteries. A different assumption on the battery storage required or a different mass of the locomotion system effects this parameter. Figure 8 shows the results of varying this parameter. It shows that a variation in the weight of the locomotion system significantly affects the operational time per day.

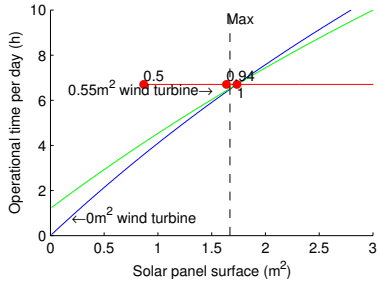

Fig. 8: A variation of Fig. 3 with the addition of the red line that shows how point A moves with variations of the mass of the locomotion system m_l, the red dots represent values of 0.5, 0.76 and 1 multiplied by the value used in the study

Furthermore, it is interesting to note the effect of varying the specific resistance (ϵ) and maximum speed (v). Varying these parameters directly scales the operational time.

5.1 Discussion of the results

From the generalisation of the study, it can be seen that a variation of assumptions for one parameter has significantly more impact on the benefit of a wind turbine and the total operational time than another parameter. Perhaps the most significant differences can be expected when the amount of solar energy turns out to be much lower (which, of course, has a negative effect) than assumed or the wind turbine turns out to be be much lighter than assumed (which has a positive effect). Furthermore, it can be seen that a variation in the mass of the solar panels has - perhaps surprisingly - little effect. Finally, variations in the weight of the locomotion system, including batteries show that a reduction of the weight seems to pay of quite well in terms of operational time.

Based on the results, one could also estimate the distance that can be traversed on a flat terrain in a day by multiplying the operational time per day with the velocity of locomotion, which is $1ms^{-1}$ in this study.

6 Conclusion

In this work, the application of robots as components of an early warning system for the Dutch flood defence system was presented with a exploratory study on

an energy-autonomous dyke robot. Based on this work, three conclusions can be drawn.

Firstly, even if only some assumption may prove valid, it is realistic to have an energy-autonomous walking dyke robot in the Netherlands. In much of the world, the amount of energy that can be harvested from the sun is significantly higher than in the Netherlands which would result in an even higher operational time.

Secondly, the use of solar panels is probably not feasible if the amount of solar energy that is available is much less than assumed in the study. However, current developments in the efficiency of solar cells will probably lead to significant improvements in the feasible operational time.

Finally, for a wind turbine, the following can be concluded: in this case study, the inclusion of a wind turbine typically offers a slight benefit. Maybe more importantly, it gives a significant benefit in the months where the incident power of the sun is low, thus allowing a reasonable operational time during the winter.

References

1. Betz, A.: Introduction to the Theory of Flow Machines. Pergamon (1966)
2. Gabrielli, G., von Karman, T.H.: What price speed?: specific power required for propulsion of vehicles (1950)
3. Green, M., Emery, K., Hishikawa, Y., Warta, W., Dunlop, E.: Solar cell efficiency tables (version 40). Progress in photovoltaics: research and applications pp. 606–614 (2012)
4. Greenman, J., Holland, O., Kelly, I., Kendall, K., McFarland, D., Melhuish, C.: Towards robot autonomy in the natural world: a robot in predator's clothing. Mechatronics 13(3), 195–228 (Apr 2003)
5. Gregorio, P., Ahmadi, M., Buehler, M.: Design, control, and energetics of an electrically actuated legged robot. IEEE transactions on systems, man, and cybernetics. 27(4), 626–34 (Jan 1997)
6. Huleihil, M.: Maximum windmill efficiency in finite time. Journal of Applied Physics 105(10), 104908 (2009)
7. Inglis, D.R.: A windmills theoretical maximum extraction of power from the wind. American Journal of Physics 47(5), 416 (1979)
8. KNMI: Jaaroverzicht van het weer in nederland - 2010. Tech. rep., KNMI (2010)
9. KNMI: Jaaroverzicht van het weer in nederland - 2011. Tech. rep., KNMI (2011)
10. KNMI: Jaaroverzicht van het weer in nederland - 2012. Tech. rep., KNMI (2012)
11. KNMI: Jaaroverzicht van het weer in nederland - 2013. Tech. rep., KNMI (2013)
12. Mart, A., Arajo, G.: Limiting efficiencies for photovoltaic energy conversion in multigap systems. Solar Energy Materials and Solar Cells 43(1996), 203–222 (1996)
13. Melhuish, C., Ieropoulos, I., Greenman, J., Horsfield, I.: Energetically autonomous robots: Food for thought. Autonomous Robots 21(3), 187–198 (May 2006)
14. Poulakakis, I., Smith, J., Buehler, M.: Modeling and experiments of untethered quadrupedal running with a bounding gait: The scout II robot. The International Journal of Robotics Research 24(4), 239–256 (Apr 2005)
15. Solbian: Solbian (2013), www.solbian.eu
16. Stine, W.B., Geyer, M.: Power From The Sun (2012), http://www.powerfromthesun.net/